processes

MDPI

Article

Exploring Exergy Performance in Tetrahydrofuran/Water and Acetone/Chloroform Separations

Jonathan Wavomba Mtogo [1,2,*], Gladys Wanyaga Mugo [2], Petar Sabev Varbanov [3], Agnes Szanyi [1] and Péter Mizsey [4,*]

[1] Department of Chemical and Environmental Process Engineering, Budapest University of Technology and Economics, 1111 Budapest, Hungary
[2] Chemical Engineering Division, Kenya Industrial Research and Development Institute, P.O. Box 30650, Nairobi 00100, Kenya
[3] Sustainable Process Integration Laboratory—SPIL, NETME Centre, FME, Brno University of Technology—VUT Brno, Technická 2896/2, 616 69 Brno, Czech Republic
[4] Advanced Materials and Intelligent Technologies Higher Education and Industrial Cooperation Centre, University of Miskolc, 3515 Miskolc, Hungary
* Correspondence: jmtogo@edu.bme.hu (J.W.M.); kemizsey@uni-miskolc.hu (P.M.)

Abstract: Distillation is significantly influenced by energy costs, prompting a need to explore effective strategies for reducing energy consumption. Among these, heat integration is a key approach, but evaluating its efficiency is paramount. Therefore, this study presents exergy as an energy quality indicator, analyzing irreversibility and efficiencies in tetrahydrofuran/water and acetone/chloroform distillations. Both systems have equimolar feed streams, yielding products with 99.99 mol% purity. The simulations are performed using Aspen Plus™, enabling evaluation at the column level, as a standalone process, or from a lean perspective that considers integration opportunities with other plants. The results show that, despite anticipated energy savings from heat integration, economic viability depends on pressure sensitivity. The results demonstrate that heat-integrated extractive distillation for acetone/chloroform raises utility energy consumption. Exergy calculations comparing standalone and total site integration reveal the variation in distillation efficiency with operation mode. Global exergy efficiency in both extractive and pressure-swing distillation depends on the fate of condenser duty. In heat-integrated extractive distillation, global exergy efficiency drops from 8.7% to 5.7% for tetrahydrofuran/water and 11.5% to 8.3% for acetone/chloroform. Similarly, heat-integrated pressure-swing distillation sees global exergy efficiency decrease from 34.2% to 23.7% for tetrahydrofuran/water and 9.5% to 3.6% for acetone/chloroform, underscoring the nuanced impact of heat integration, urging careful process design consideration.

Keywords: heat integration; process intensification; computer modeling; distillation energy efficiency; environmental impact; thermodynamic efficiency

check for updates

Citation: Mtogo, J.W.; Mugo, G.W.; Varbanov, P.S.; Szanyi, A.; Mizsey, P. Exploring Exergy Performance in Tetrahydrofuran/Water and Acetone/Chloroform Separations. *Processes* **2024**, *12*, 14. https://doi.org/10.3390/pr12010014

Academic Editors: Jesus Rafael Alcantara-Avila, Julián Cabrera Ruiz, Yuhe Tian and Elio Santacesaria

Received: 2 November 2023
Revised: 30 November 2023
Accepted: 17 December 2023
Published: 20 December 2023

1. Introduction

Despite distillation being a well-known and most widely exploited separation technology throughout the chemical industry, it is generally associated with significant energy consumption. Up to 95% of all liquid separations within the chemical industry are implemented using distillation, accounting for about 3% of the total energy consumption in the world [1]. This energy comes mostly from fossil sources which are limited and their use has potential environmental consequences. Reducing the energy consumption of the distillation can be clearly translated into CO_2 emission reduction [2,3]. That motivates the research and engineering interest in improving the efficiency of distillation. Several energy-saving technologies, such as partial heat integration [4], full heat integration [5], thermal coupling [6], heat pump [7], side-stream [8], and intermediate reboiler [9] are implemented to reduce energy consumption in the distillation processes.

The most commonly used technique is heat integration. The core principle of heat integration is the heat exchange between the hot and the cold process streams. The initial proposal for heat integration was made by Linnhoff and Flower [10] after realizing the potential for energy savings through the design of heat exchanger networks and pinch analysis. Commonly, when performing process optimization with heat integration, a sequential approach is used. Initially, the process is optimized under the assumption that all heating and cooling loads are supplied by utilities. Heat integration is then carried out after the optimal stream conditions, such as flow rates, temperatures, and pressures, are identified [11]. There are several heat integration flowsheets, including partial heat integration [12] and full heat integration [13].

Heat integration has been applied to special distillation processes for separating azeotropic mixtures. These include extractive distillation [14] and pressure-swing distillation [15]. Extractive distillation requires properly selected solvents that have to be regenerated and recycled, whereas pressure-swing distillation is applied in the case of pressure-sensitive components. Extractive and pressure-swing distillation processes are used for the recovery of solvents from waste streams as a way of environmental protection. Coupled with heat integration, this makes the two special distillation processes attractive. The potential for heat integration in pressure-swing distillation is an inherent feature [16]. However, there is a need to increase pressure in one of the columns to achieve a sufficient temperature difference for heat integration in extractive distillation [17]. This approach makes it comparatively less favorable to undertake heat integration in extractive distillation.

In the case of pressure-swing distillation of a binary azeotrope, two columns operate at different pressures. One column is the low-pressure column and the other column is the high-pressure column. Backward heat integration is usually carried out for minimum-boiling azeotropes and forward heat integration is carried out for maximum-boiling azeotropes. In full heat integration, the condenser duty of the high-pressure column should be made equivalent to the reboiler duty of the low-pressure column [18]. Such a heat integration enables the HPC to heat up the LPC. It has been shown that heat integration results in the reduction of energy consumption by up to 40% but with a trade-off in controllability [5]. Heat integration in this manner relies on the first law of thermodynamics and heat energy balance around the distillation process. The energy balance, however, does not distinguish between different types of energy and does not account for losses brought on by the decline in the quality of the energy.

To get around this drawback, it is possible to conduct an exergy analysis to determine the thermodynamic efficiency of a process. Exergy analysis is rooted in the principles of the second law of thermodynamics, which considers the actual work involved in separation processes and aids in understanding the quality of energy [19]. By employing exergy analysis, it becomes feasible to quantitatively assess the quality of different energy flows within a system, allowing for a comprehensive evaluation of all key aspects of energy utilization. Exergy, also known as availability, represents the maximum amount of work that a system can accomplish when it is brought into thermodynamic equilibrium with the environment in reversible mode [20]. The heat source, the heat sink, and the thermodynamic pathways are related to the process. Thus, exergy is inclusive of the total system including the state of the reservoir. In this manner, the quality of the energy form is considered. Another related measure is exergy efficiency. This is defined as the separation work performed divided by the total available exergy. It expresses the fraction of the available work capacity that the system is able to utilize. These thermodynamic analyses provide a tool for identifying and quantifying inefficiencies in individual processes.

Exergy and exergy analysis have been studied in distillation systems. Zemp et al. [21] studied the driving forces profile of the distillation columns and established the exergy loss profile. Sauar et al. [22] investigated and compared the efficiency of binary distillation columns using the equal thermodynamic distance and equipartition of forces methods. Seyed et al. [23] provided a methodology for analyzing the exergy of distillation columns using driving forces. Haragovics [24] used exergy analysis to evaluate distillation structures from the perspective of lean manufacturing. They investigated plain distillation structures with boundaries around the core process and of a standalone system. They also considered a backward heat-integrated configuration without recycle flows. Demirel [25] provided an extensive derivation of the underlying thermodynamic equations and a thorough overview of conventional techniques for thermodynamic analysis with an emphasis on distillation operations. Yuan et al. [26] carried out an exergy analysis for the triple-column extractive distillation process for the separation of a ternary azeotropic mixture. Javed et al. [27] investigated exergy losses in internally heat-integrated distillation columns, externally heat-integrated double distillation columns, and vapor recompression systems applied to the separation of i-butane and n-butane. Guerrero-Martin et al. [28] conducted a study on the exergy load distribution analysis in a separation procedure using extractive distillation for the dehydration of ethanol.

Although there have been several applications for distillation-based separations, the exergetic loss in pressure-swing distillation with mass and energy integration has only been briefly discussed in a few publications. Zhao et al. [29] investigated the separation of the ternary multi-azeotropes system of di-isopropyl ether/isopropanol/water via reactive pressure-swing distillation and extractive distillation. Their results showed that reactive pressure-swing distillation was better than reactive extractive distillation in terms of economy, environment, and exergy performance. Also, the separation of acetonitrile/isopropanol/water ternary mixture through a heat-integrated reactive coupling pressure-swing distillation process has been studied [9].

In a previous study [5], the separation processes of binary azeotropic mixtures of tetrahydrofuran/water and acetone/chloroform were investigated with a focus on energy efficiency and controllability. The processes were specifically designed to achieve high-purity products and were optimized accordingly. Through the implementation of full heat integration, the objective of reducing energy consumption and lowering costs was accomplished. The evaluation of energy conservation performance was conducted by considering total energy consumption. Mangili et al. [30] applied the exergy analysis method to the THF/water designs by Ghughe et al. [31]. They calculated the exergetic performance of heat-integrated alternatives. No calculations for the non-heat-integrated alternatives were presented. The exergy calculations that exist in the literature assume that the exergy outflow from the condensers is used in subsequent processes. However, it is possible to encounter situations where a waste heat stream at the required temperature is not readily accessible within a plant. Similarly, the temperature of the heat obtained from a condenser may not be suitable for advantageous utilization elsewhere in the plant. When the condenser duty cannot be employed elsewhere in the plant, it is ultimately released into the environment, resulting in the loss of its exergy benefit. Based on the review of existing literature, it is important to highlight that the exergy analysis method, which takes into account the ultimate utilization of the condenser duty, has not been applied in the direct full heat integration of the tetrahydrofuran/water system. Furthermore, the exergetic performance of acetone/chloroform separation through extractive and pressure-swing distillation has not been assessed.

The aim of this paper is to determine the feasibility of employing heat-integrated configurations, specifically in ED and PSD, for the separation of minimum-boiling and maximum-boiling azeotropes. Additionally, we seek to compare the performance of heat-integrated ED and PSD alternatives with conventional ED and PSD alternatives, taking into consideration the fate of the condenser duty. The objective is to bring clarity and certainty to these aspects, providing valuable insights into the advantages of heat-integrated ED and PSD options. The exergy destruction of each individual column as well as the overall systems is investigated. Additionally, a comparative analysis is conducted to assess the thermodynamic efficiencies of both non-heat-integrated and fully heat-integrated alternatives. The research also aims to explore the flexibility dimension within lean manufacturing, and present a comprehensive examination of exergy analysis to reveal the exergy reserves in a distillation system.

2. Exergy Analysis of Distillation Columns

The evaluation of the thermodynamic efficiency of any separation process can be achieved through the calculation of performance indices. Exergy analysis is an effective tool for process optimization [32,33] and measures the quality and efficiency of energy use. Araújo et al. [34] presented an exergy analysis of an industrial case study on the purification of 1,2-ethylene dichloride in a high-purity distillation column. They found that utilizing a vapor recompression heat pump results in a significant improvement in energy utilization by lowering the irreversibility rate of the condenser. Le Goff et al. [35] undertook exergy analysis for efficiency comparison between the conventional and diabatic distillation processes for separating an ammonia–water mixture. Their results showed that the diabatic distillation column halves the exergy loss of a conventional distillation column.

Exergy analysis may also be employed to examine complex distillation plants and identify areas of the processes where there are substantial exergy losses and improvements are feasible. Exergy analysis was utilized by Yan et al. [36] to identify vital points where improvements could be carried out. Therefore, exergy analysis was the foundation for our study. A separation process within a specified system boundary can be depicted in Figure 1. The system is isolated from the environment which is the surrounding reservoir. The environment has a reference temperature T_o and a reference pressure P_o.

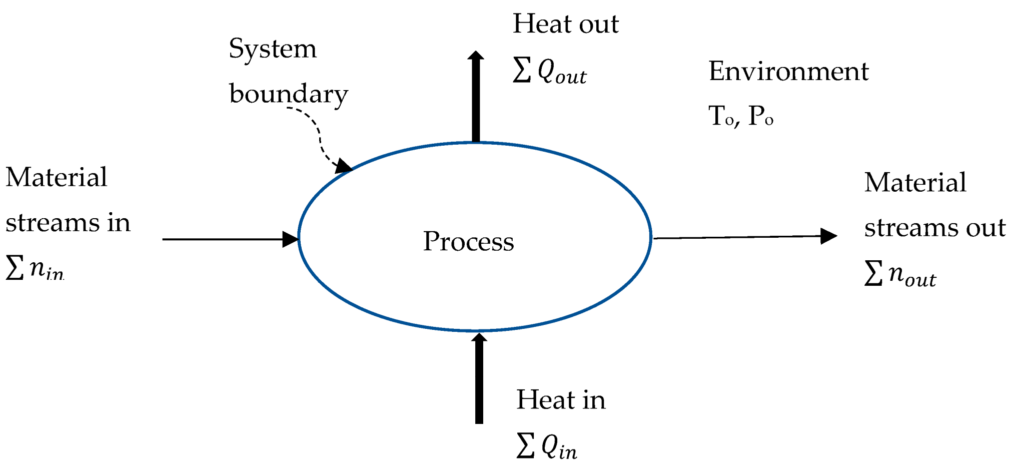

Figure 1. A schematic representation of a separation process with material streams and heat energy streams relative to the environment.

Components mixing is a spontaneous irreversible process that generates entropy, whereas the ideal separation of a mixture could be perceived as a reverse mixing process that is accomplished through external work. Similarly, the distillation process is associated with a great amount of heat and mass transfer. Since real distillation processes have a finite number of trays and limited number of point-like heat transfers, the processes are irreversible. Therefore, there is exergy loss in the reboiler, condenser, and trays. Rivero and Anaya [37] defined the exergy content of a stream as

$$Ex = (H - H_o) - T_o(S - S_o) \tag{1}$$

where H and S represent specific enthalpy and the specific entropy of a stream at system conditions, and H_o and S_o are the enthalpy and entropy at the reference temperature T_o and 1 bar pressure. In this work, T_o is considered to be 303.15 K.

Figure 2 shows the inlet and outlet streams of a simple column. The sum of exergy lost at every stage represents the exergy loss of the column (Ex_{col}), and can be estimated as follows:

$$Ex_{col} = \Sigma(Ex_{in}) - \Sigma(Ex_{out}) \tag{2}$$

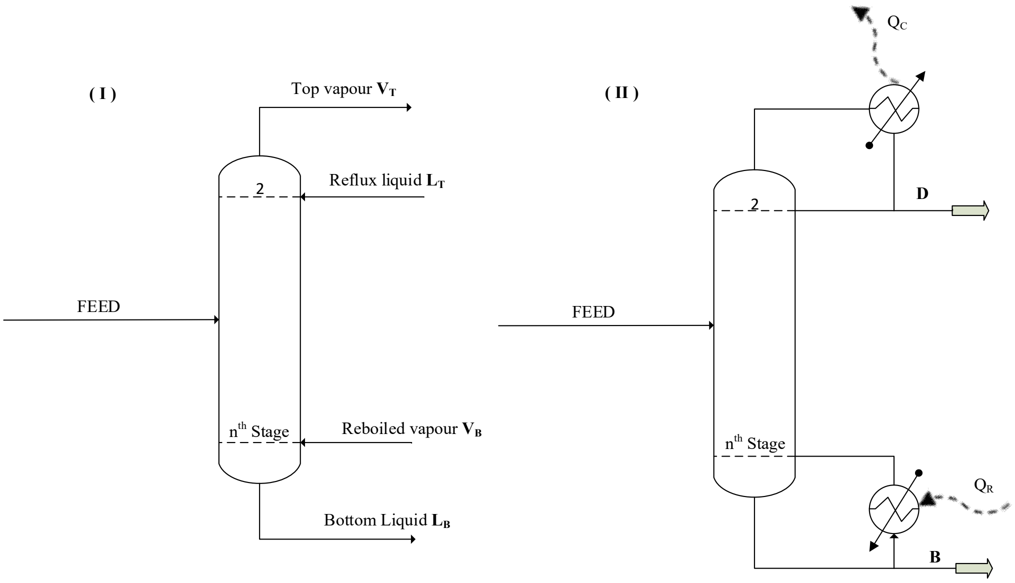

Figure 2. Input and output streams of a distillation column without (**I**) and with heat exchangers (**II**).

Equation (2) can be calculated using the following formula:

$$Ex_{col} = (H_F + H_{LT} + H_{VB} - H_{VT} - H_{LB}) - T_o(S_F + S_{LT} + S_{VB} - S_{VT} - S_{LB}) \quad (3)$$

The exergetic loss in the reboilers and condensers is calculated from their respective exergy balance which can be expressed by

$$n_{in}Ex_{in} = Q_c\left(1 - \frac{T}{T_c}\right) + n_{out}Ex_{out} \quad (4)$$

$$n_{in}Ex_{in} = Q_R\left(1 - \frac{T}{T_R}\right) + n_{out}Ex_{out} \quad (5)$$

where n_{in} and n_{out} are the stream molar flows and Ex_{in} and Ex_{out} are the stream molar exergy. The reboiler provides high-quality heat (Q_R, T_R) which is removed from the top in low-quality form (Q_C, T_C) by the condenser. This causes the energy to degrade, in a similar manner to a heat engine. The separation of the pure components is achieved through work provided by the utility system. When a distillation column is compared to a reversible heat engine, presuming that the temperature of the cold and hot utility is constant, the net utility work consumption can be calculated by

$$W_{net} = Q_R\left(1 - \frac{T}{T_R}\right) - Q_c\left(1 - \frac{T}{T_c}\right) \quad (6)$$

The separation work for a distillation column is equal to the exergy difference between the feed streams and the product streams [38].

$$W_{sep} = \Sigma_{out}(n \times Ex) - \Sigma_{in}(n \times Ex) \quad (7)$$

where n is the mole flow rate of the feed and the product streams.

For a completely reversible distillation process, the utility system must provide work equivalent to the minimum separation work. Exergy loss, however, exists in any real process because of the variations in temperature and stream composition that mix at the various locations in the column. The minimum separation work must always be lower than the amount of work consumed by the utility. Then, from the availability balance, the total exergy loss can be calculated.

$$Ex_{loss} = \Sigma_{in}\left[n \times Ex + Q\left(1 - \frac{T_o}{T_R}\right)\right] - \Sigma_{out}\left[n \times Ex + Q\left(1 - \frac{T_o}{T_c}\right)\right] \tag{8}$$

The efficiency is finally determined by dividing the minimum amount of useful work by the total amount of energy input.

$$\eta = \frac{W_{sep}}{W_{sep} + Ex_{loss}} \tag{9}$$

Initiatives have been made to devise distillation techniques that consume less energy. Nevertheless, the economic situation and the energy-saving approach employed can potentially impact the overall efficiency of a plant. Many design calculations are based on the assumption that the system will operate optimally under ideal conditions. However, in reality, industrial facilities are constructed to have a lifespan of several decades, during which market dynamics may change and new manufacturing facilities may be established and interconnected. It becomes crucial to consider the implications when plants are no longer interconnected. Does a prolonged shutdown of a linked plant have an impact on the exergy efficiency of the operational plant? Exploring this effect is essential to gain a comprehensive understanding of the situation.

3. Case Studies

3.1. THF/Water Separation Using Extractive Distillation

The first case study is the tetrahydrofuran dewatering process, whose significance has been well established in the literature [39,40]. At atmospheric pressure, tetrahydrofuran (THF) has a boiling point of 65.97 °C and water has a boiling point of 100 °C. THF and water form a minimum boiling homogeneous azeotrope with a boiling point of 63.43 °C and an azeotropic composition of 82.87 mol% of THF. The most common extractive distillation has two columns, the extractive column (EC) and the solvent regeneration column (SRC). The binary feed mixture and the entrainer (DMSO) enter the EC at different trays. The entrainer breaks the azeotrope. The overhead product is THF with trace impurities. The bottom stream then enters the SRC. High-purity water is distillated at the top and a high-purity entrainer is discharged at the bottom. After cooling down, the entrainer is recycled back to the EC. A small quantity of makeup entrainer equivalent to the entrainer loss is added.

From the literature, there already exists a good design for the ED process of THF dehydration [31]. In the design, the binary feed was 100 kmol/h of equimolar THF/water composition. Both the distillate product purities were set at 99.99 mol%. The thermodynamic property model used was NRTL with Aspen Plus in-built binary parameters chosen for its good agreement with experimental results as shown by Zhang et al. [41]. Sensitivity analysis was implemented for optimization of process parameters with the objective of minimizing total annual cost (TAC). However, this process had been designed without taking into account the pressure drop per tray, which is a key parameter in distillation. Also, the pressure selection had not been optimized. The selection of distillation pressure significantly impacts energy costs, emphasizing the vital significance of column pressure as a key variable in optimizing distillation process design. An improvement to the design was undertaken by Gu et al. [42] who considered a tray pressure drop of 0.0068 bar. This resulted in an increase in TAC by 4%, underscoring the importance of tray pressure drop and the pressure sensitivity of the azeotrope. Additionally, they conducted the optimization of various column parameters, such as distillate rates, molar reflux ratios, feed tray positions, and entrainer flow rate, while maintaining the total number of trays in the columns. This was achieved through the minimization of full energy consumption. Therefore, in this section, we adopt the work of Gu et al. [42]. Figure 3 shows the flowsheet.

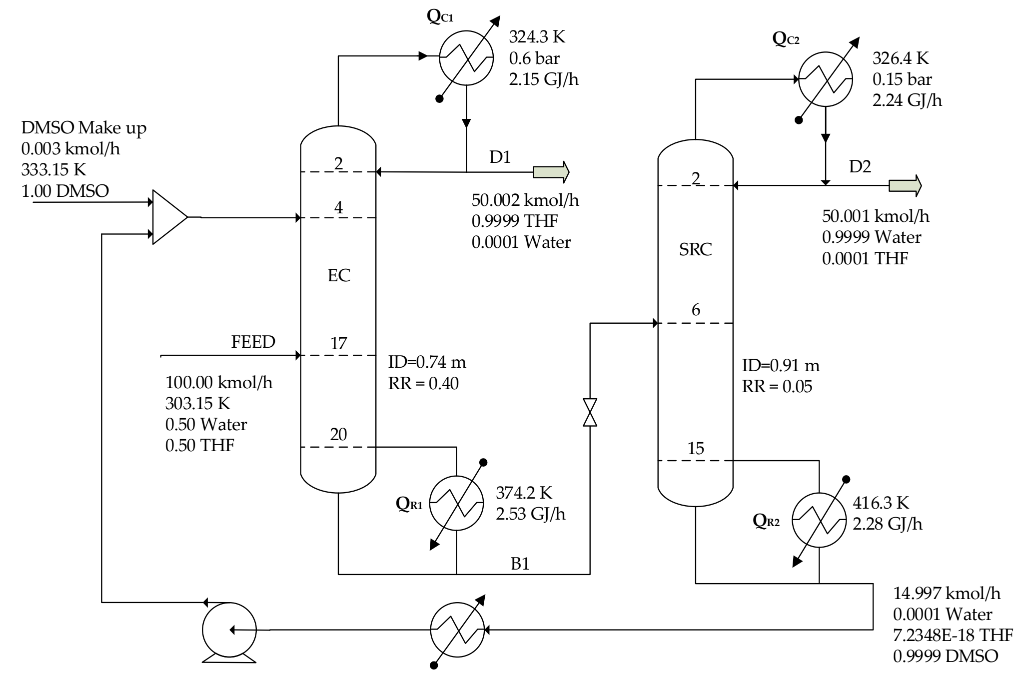

Figure 3. Structure of the conventional extractive distillation system.

Direct full heat integration for the process is carried out after optimizing the pressure of the solvent recovery column to allow a sufficient heat gradient and minimum TAC. The operating pressure of EC is 0.6 bar which gives a top temperature of 324.3 K and a reboiler temperature of 374.2 K. For the operating pressure of 0.15 bar of the SRC, the top temperature is 326.4 K and the reboiler temperature is 416.3 K. A pressure optimization by Gu et al. [42] gave an operating pressure of 2 bar in the SRC as the optimal for direct full heat integration. At 2 bars, the top temperature of SRC is 392.8 K and the reboiler temperature is 374.2 K. This provided a temperature difference of 18.6 K for heat integration. The implementation of heat integration is performed using the Design Spec tool in Aspen Plus, where RR_2 is defined as a variable and $Q_{R1} - Q_{C2} = 0$ is specified as a requirement. With these conditions, RR_2 has to be increased from 0.05 to 0.27, with the corresponding increase in the reboiler heat duty from 2.28 to 3.04 GJ/h. Figure 4 shows the flowsheet.

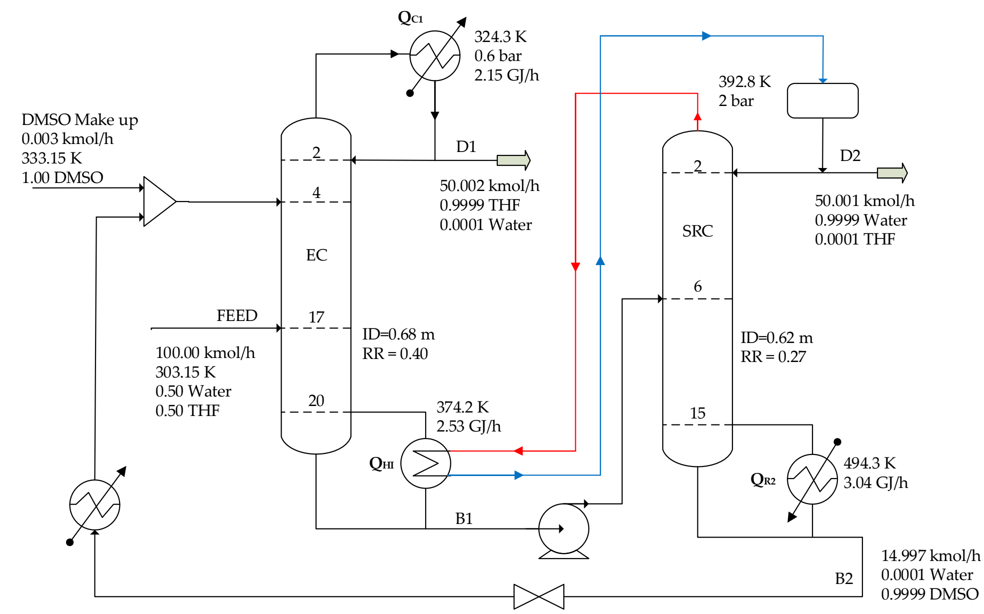

Figure 4. Structure of the conventional extractive distillation system with heat integration.

3.2. Acetone/Chloroform Separation Using Extractive Distillation

The separation of acetone and chloroform through extractive distillation has been investigated by various authors. The authors of [43] used methyl-n-pentyl ether as the entrainer for the separation, to demonstrate heuristics and mathematical modeling insights for process design. Luyben [44] added dimethyl sulfoxide (DMSO) as the heavy entrainer to improve the relative volatility of acetone over chloroform. His work showed that DMSO lowered equipment cost and improved product purity to 99.5 mol%. Other authors employed different entrainers such as ethylene glycol [44] and N-methyl-2-pyrrolidone [45]. For this study, the acetone/chloroform flowsheet is adapted from the work of Luyben [44]. The design is reoptimized for 99.99 mol% product purity. The fresh feed constitutes 50 mol% acetone and 50 mol% chloroform with a flow rate of 100 kmol/h. The pure DMSO flow rate is 164.4 kmol/h. The design is given in Table 1.

Table 1. Acetone/chloroform extractive distillation process parameters.

		EC	SRC
Total number of theoretical plates		32	15
Feed rate (kmol/h)		100.0	214.4
Binary feed stage		13	5
Solvent feed stage		4	
Pressure (bar)		1.1	1.1
Molar reflux ratio		1.70	0.69
X_D	Acetone (mol%)	99.99	0.01
	Chloroform (mol%)	0.01	99.99

As far as we know, there is no available literature on direct full heat integration on the extractive distillation of this azeotrope. However, partial heat integration has been undertaken where the bottom stream of the solvent recovery column is used to preheat the feed [45]. For this work, direct full heat integration is implemented for the optimized conventional ED process. From Table 1, the operating pressure in both columns is 1.1 bar, resulting in corresponding temperatures of 415 K at the bottom of the extractive column (T_{R1}) and 337.3 K at the top of the solvent recovery column (T_{C2}). However, due to the lack of temperature driving force from the solvent recovery column to the extractive column, heat integration is not possible. To establish the required temperature driving force, the operating pressure of the solvent recovery column (P_2) needs to be increased. A sensitivity analysis is conducted by varying P_2 while adjusting the reflux ratio of the solvent recovery column (RR_2) to meet the purity requirements of the products. At P_2 = 10 bar, T_{R1} = 415 K, and T_{C2} = 427.4 K, a temperature gradient of only 12.4 K is achieved. This observation aligns with the low-pressure sensitivity of the acetone/chloroform azeotrope. To enable heat integration, the reboiler of the extractive column is heated by the heat from the condenser of the solvent recovery column, which is achieved by adjusting the pressure of the solvent recovery column (P_2) to provide the necessary temperature driving force. The heat integration process is implemented using the Design Spec tool in Aspen Plus. The reflux ratio of the solvent recovery column (RR_2) is set as a variable, and the heat duty of the reboiler (Q_{R1}) is set equal to the heat duty of the condenser (Q_{C2}) as a specification.

3.3. THF/Water Separation Using Pressure-Swing Distillation

From the literature, there already exists a good design for the PSD process of THF dehydration [31]. The process consists of a binary equimolar feed mixture of THF and water. The total feed is 100 kmol/h at 303.2 K and the purity specifications are 99.99 mol%. There are two columns that are operated at different pressures. The first column is a low-pressure distillation column (LPC) while the second column is a high-pressure distillation column (HPC). The composition of the distillate of the first column is the azeotropic composition at low pressure while the composition of the distillate of the second column is the azeotropic composition at high pressure. The detailed setting of the thermodynamic model with binary

NRTL interaction parameters can be found in Supplementary Materials. The corresponding T-x-y diagram can be found in our previous work [5]. Figure 5 gives a steady-state flowsheet that has been simulated and optimized in Aspen Plus V10 software. Ghuge et al. [31] also provided the flowsheet for direct full heat integration for the process, shown in Figure 6. A tray pressure drop of 0.0068 bar is considered.

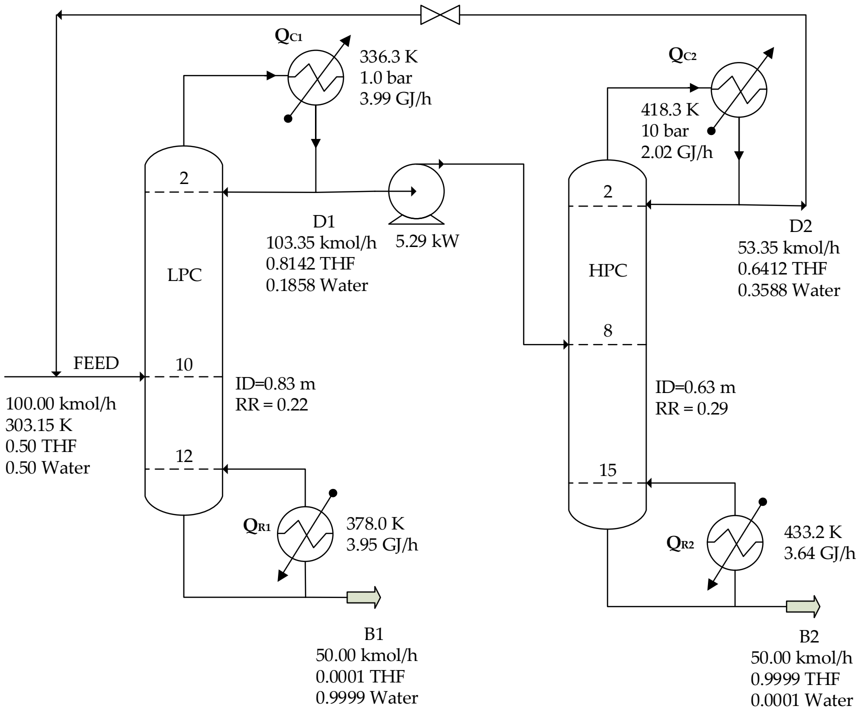

Figure 5. Structure of the conventional pressure-swing distillation system.

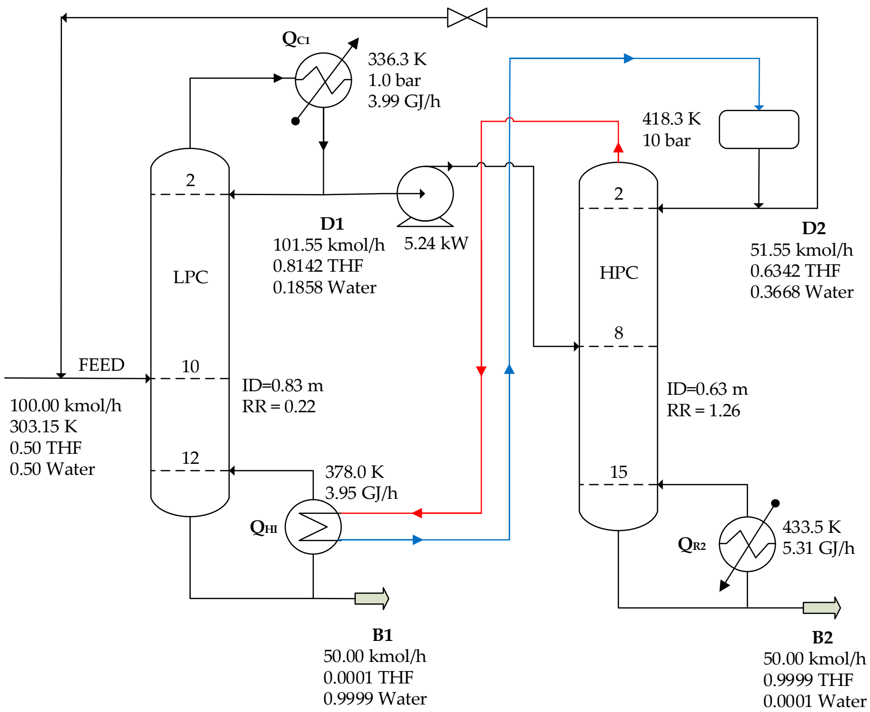

Figure 6. Structure of the conventional pressure-swing distillation system with heat integration.

3.4. Acetone/Chloroform Separation Using Pressure-Swing Distillation

The column configuration for the separation of the maximum-boiling acetone/chloroform azeotrope is different from the THF/water configuration. In this system, the first column is the HPC, whereas the second column is the LPC. The products are distillates. The mixture is fed into the HPC which produces high-purity acetone in its top stream D_1. The bottom stream B_1 is depressurized into the LPC which produces high-purity chloroform in its top stream D_2. The bottom stream B_2 of the LPC is the azeotrope. Stream B2 is recycled to the HPC. The same feed conditions and product purity constraints were used. Through adjusting the pressure of the two columns, the azeotropic concentration is crossed for effective separation. The HPC is operated at 10.69 bar and the LPC is at 0.75 bar. The corresponding T-x-y diagram can be found in our previous work [5]. The acetone/chloroform flowsheet is adapted from Yang et al.'s work [46] where the UNIQUAC thermodynamic model was used because it fits well with experimental vapor liquid equilibrium data [47]. The design is reoptimized for 99.99 mol% product purity. Table 2 shows the process parameters.

Table 2. Acetone/chloroform process parameters.

		HPC	LPC
Total number of theoretical plates		82	43
Feed rate (kmol/h)		100.0	620.3
Binary feed stage		21	21
Recycle feed stage		51	
Pressure (bar)		10.69	0.75
Molar reflux ratio		27.63	19.81
X_D	Acetone (mol%)	99.99	0.01
	Chloroform (mol%)	0.01	99.99

4. Results

4.1. Effect of Heat Integration

The effect of heat integration on the distillation systems was explored in conventional extractive distillation and conventional pressure-swing distillation. Direct full heat integration for extractive distillation is premised on integrating the top vapor of the second column to heat up the bottoms of the first column, which requires raising the pressure of the second column. As a result, suitable pressure and heat duty selection is a component of the design problem. However, pressure-swing distillation has an inherent feature for heat integration. The energy consumption for the systems is shown in Table 3.

Table 3. Energy consumption.

	Energy Consumptions GJ/h			
	ED	**DFHIED**	**PSD**	**DFHIPSD**
THF/Water (Mix 1)	4.81	3.04	7.59	5.31
Acetone/Chloroform (Mix 2)	10.60	12.47	69.96	36.94

Direct full heat integration for the conventional extractive distillation of the minimum boiling THF/water azeotrope results in the reduction of energy consumption from 4.81 to 3.04 GJ/h. This represents an energy reduction of 36.8%. A reduction of energy consumption from 7.85 to 5.31 GJ/h (a reduction of 32.4%) is also achieved in the direct full heat-integrated pressure-swing distillation of THF/water. For the direct full heat-integrated extractive distillation of the maximum-boiling acetone/chloroform azeotrope, there is instead an increase in energy consumption. For this case, energy consumption increases from 10.60 to 12.47 GJ/h (an increase of 15.0%). This is because of the lower pressure sensitivity of the azeotrope. We can conclude that DFHIED for acetone/chloroform is infeasible. However, DFHIPSD for acetone/chloroform is feasible. There is an energy consumption reduction from 69.96 to 36.94 GJ/h (a reduction of 47.0%). DFHIPSD for acetone/chloroform was achieved in forward heat integration using the HPC-LPC configuration.

4.2. Exergetic Analysis

It is vital to specify the boundaries of the system under consideration when undertaking thermodynamic analysis. Column and system boundaries are applied in this study. Column boundaries take into account the thermodynamic performance of each distillation column. System boundaries, on the other hand, take into account the thermodynamic performance of any auxiliary equipment such as feed preheaters and product coolers. The blue dashed lines represent column boundaries, whereas the red dashed lines represent system boundaries, as shown in Figure 7. For all configuration schemes, irreversibility rates and thermodynamic efficiencies are computed based on the equations above. Efficiency calculations are made using the procedures suggested by Kotas [48] and the calculations for the stream exergies are performed using the procedure suggested by Hinderink et al. [49]. All the thermodynamic properties are obtained from the Aspen Plus™ simulations. Table 4 shows the exergy details of each distillation configuration for the azeotropic systems. The values are for calculations around the core process and the units are in kW.

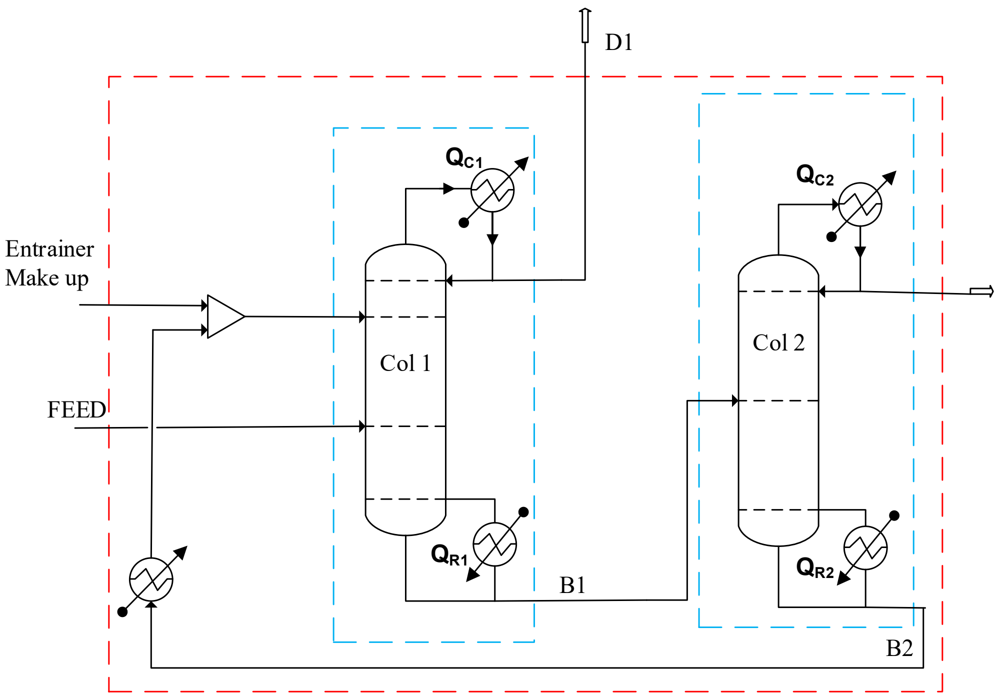

Figure 7. System boundaries for thermodynamic analysis.

The core process has boundaries around the distillation columns themselves and considers the thermodynamic performance of the system. The exergy of a stream not leaving the system is not shown. The heat duties of the condenser can be used in other units in the industrial setup.

In order to determine the major source of irreversibility, Table 5 shows the thermodynamic evaluations for every unit individually. Subsequently, the exergetic losses attributed to each piece of equipment are calculated using Equation (8), whereas the global exergy efficiency of each process is calculated using Equation (9). $\dot{E}x_{dest}$ represents the internal exergy loss rate in kW and is calculated as the difference between total exergy in and total exergy out. $\dot{E}x_{dest}$ is calculated using Equation (10) [48]. In Table 5, η is the thermodynamic efficiency in percentage.

$$\dot{E}x_{dest} = \Sigma_{in}(Ex) - \Sigma_{out}(Ex) \tag{10}$$

Table 4. Details of exergy of each distillation configuration (units in kW).

	ED Mix 1	DFHIED Mix 1	ED Mix 2	DFHIED Mix 2	PSD Mix 1	DFHIPSD Mix 1	PSD Mix 2	DFHIPSD Mix 2
Ex_{reb1}	133.5	0.0	517.4	0.0	213.2	0.0	3969.8	3969.8
Ex_{reb2}	172.1	326.5	365.2	1653.7	283.9	443.2	663.6	0.0
Ex_{reb_total}	305.7	326.5	882.6	1653.7	497.1	443.2	4633.4	3969.8
Ex_{cond1}	38.8	38.8	96.6	96.6	110.8	108.9	2843.5	0.0
Ex_{cond2}	44.4	0.0	69.2	0.0	154.6	0.0	609.1	875.5
Ex_{cond_total}	83.2	38.8	165.8	96.6	265.5	108.9	3452.6	875.5
Ex_{cooler}	4.6	9.8	89.3	183.1	0.0	0.0	0.0	0.0
Ex_{HX_in}	0.0	160.5	0.0	558.1	0.0	301.6	0.0	2843.5
Ex_{HX_out}	0.0	133.5	0.0	517.4	0.0	216.9	0.0	1071.8
$Ex_{loss\ HX}$	0.0	27.0	0.0	40.7	0.0	84.7	0.0	1771.7
$Ex_{loss\_utility}$	217.9	250.9	627.5	1414.7	231.6	418.9	1180.8	4866.0
Ex_{pump}	0.1	0.1	0.1	0.1	5.3	5.2	21.0	21.0
Ex_{Feed}	0.0	0.0	0.0	0.0	0.0	0.0	2.8	2.8
Ex_{Makeup}	0.0	0.0	0.0	0.0	0.0	0.0	0.0	0.0
Ex_{D1}	1.9	1.9	3.4	3.4	9.0	7.9	48.7	48.5
Ex_{D2}	1.0	13.3	4.1	45.8	73.0	39.3	1.9	2.2
Ex_{B1}	14.0	14.0	152.4	152.4	20.6	9.4	720.7	720.4
Ex_{B2}	10.6	30.3	255.8	720.0	56.8	60.3	55.9	55.5
Ex_{loss_stream}	27.5	59.6	415.7	921.7	159.4	117.0	824.4	823.9
Ex_{in}	305.7	326.6	882.6	1653.7	497.1	443.2	4636.2	3972.6
Ex_{out}	86.1	54.0	262.6	328.9	342.9	178.7	3503.2	926.3
$Ex_{destruction}$	219.6	272.6	619.9	1324.8	159.5	269.8	1133.0	3048.8

Table 5. Thermodynamic evaluation results of the columns in ED.

Column	ED Mix 1		DFHIED Mix 1		ED Mix 2		DFHIED Mix 2	
	$\dot{Ex}_{dest}$	η_1	$\dot{Ex}_{dest}$	η_1	$\dot{Ex}_{dest}$	η_1	$\dot{Ex}_{dest}$	η_1
EDC	79.5	16.1	27.02	12.5	272.5	35.3	324.6	32.1
SRC	130.2	1.9	269.9	15.3	188.5	36.3	1002.2	53.7

Tables 5 and 6 show that large irreversibilities associated with the processes occur primarily in the columns in both ED and PSD technologies. In essence, the distillation columns dominate input exergy consumption, which could be attributed to the high energy-dissipating properties of distillation processes. For example, in the extractive distillation of THF/water, backward heat integration amplifies the SRC irreversibility rate, while significantly reducing the EC irreversibility rate. This is because heat integration lowers the total reboiler duty, subsequently reducing the exergy inflow rate for the reboilers. Consequently, the SRC exergy efficiency increases. From Table 5, the exergy inflow rate into the reboiler for the HIED is 19.9% less than that for the non-heat-integrated ED. When compared to non-heat-integrated ED, the exergy outflow rate from the condenser for HIED is 53.4% lower. As a consequence, the total utility exergy loss for HIED is 22.3% lower than for non-heat-integrated ED, resulting in a 25.4% reduction in the total exergy loss rate.

Table 6. Thermodynamic evaluation results of the columns in PSD.

Column	PSD Mix 1		DFHIPSD Mix 1		PSD Mix 2		DFHIPSD Mix 2	
	$\dot{Ex}_{dest}$	η_1	$\dot{Ex}_{dest}$	η_1	$\dot{Ex}_{dest}$	η_1	$\dot{Ex}_{dest}$	η_1
LPC	72.8	28.9	1.5	9.0	418.3	52.1	1490.0	17.8
HPC	9.0	93	268.3	40.3	316.7	62.9	1558.8	24.4

For the extractive distillation of acetone/chloroform, backward heat integration increases the irreversibility rate for the SRC. This is because of the large pressure required to elevate the temperature in the column in order to achieve heat integration. This results in higher reboiler heat input to the SRC. The large reboiler duty raises the exergy inlet rate significantly, resulting in a rise in the exergy destruction rate in the reboiler. The exergy inflow rate of the reboiler in HIED is 87.3% higher compared to the non-heat-integrated alternative. The exergy outflow rate of the condenser in HIED is 41.7% lower. The overall exergy loss rate for utilities in HIED is 125% greater than in non-heat-integrated ED. This is because the integrated heat exchanger raises the exergy rate for condensation.

While the decrease in exergy efficiency with heat integration might seem unexpected initially, a closer analysis clarifies the pattern. The key insight is that lower pressure systems generally exhibit higher efficiencies. This is because the boiling temperature increases with rising pressure. Since higher temperature energy holds greater exergy value, employing more valuable energy for the same separation work leads to lower efficiency at higher pressures.

Table 6 illustrates similar results. In the PSD of THF/water, direct full heat integration reduces the irreversibility rate of the LPC but raises that of the HPC. This can be attributed to the reduction in exergy rates of streams leaving the LPC and the increase in exergy inflow in the reboiler of the HPC. The exergy inlet rate to the reboiler in DFHIPSD is 10.8% lower in comparison to the non-heat-integrated option. The exergy outlet rate of the condenser is 59.0% lower than the non-heat-integrated option. The thermodynamic efficiencies of both the LPC and the HPC are reduced. It is worth noting that in this system, the products leave from the bottom of the column at comparatively higher temperatures.

The column arrangement for PSD of acetone/chloroform is HPC-LPC and the heat integration is forward heat integration. However, this integration raises the irreversibility rate of the LPC due to the integrated heat exchanger, resulting in increased exergy inflow to the LPC. While the total exergy inlet to the reboiler in DFHIPSD is 14.3% lower than the non-heat-integrated option, the exergy outlet rate of the condenser decreases by 74.6%. Nevertheless, additional exergy destruction occurs at the integrated heat exchanger. Consequently, the overall exergy loss rate of utilities for DFHIPSD is 312% higher than in the non-heat-integrated PSD.

Table 7 shows the thermodynamic efficiency for each distillation configuration. The global thermodynamic efficiency of the system exhibits inferior performance when compared to that of the individual columns, in most cases. This can be attributed to the increased irreversibility in the reboiler.

Table 7. Thermodynamic efficiency values for all distillation configurations for the four definitions.

System	ED Mix 1	DFHIED Mix 1	ED Mix 2	DFHIED Mix 2	PSD Mix 1	DFHIPSD Mix 1	PSD Mix 2	DFHIPSD Mix 2
Total exergy destruction (kW)	219.7	272.5	461.0	1324.8	81.9	269.8	1135.0	3048.8
Exergetic efficiency (%)	1.3	6.1	1.2	3.5	33.4	16.7	4.0	1.0

The global thermodynamic efficiency of the systems is lower where the distillates are the products. However, for the pressure-swing distillation of THF/water where the products are obtained from the bottom of the columns, the global thermodynamic efficiency is significantly higher. This is because the bottom products leave the columns at elevated temperatures in comparison to the systems with distillate products. Consequently, these bottom product streams leave with a higher exergy rate.

The most intriguing observation is the divergence between the results of extractive distillation and pressure-swing distillation configurations. Whereas heat integration is commonly implemented to reduce energy consumption, these results indicate that it is not necessarily the ideal solution. Heat-integrated extractive distillation shows higher global thermodynamic efficiency than its non-heat-integrated alternative. For the THF/water, the increase in thermodynamic efficiency results primarily from the decrease in the exergy loss rate of the utilities.

Also, the higher operating temperatures in the SRC increase the enthalpy of the products, which results in an increased exergy rate for the product streams. For the acetone/chloroform, heat integration results in an almost threefold increase in the global thermodynamic exergy loss. This is because of the higher pressures in the SRC. The global thermodynamic efficiency of the heat-integrated alternative decreases. This heat integration is uneconomical because it has the opposite effect of increasing energy consumption.

There is a worse performance for the heat-integrated configurations of the PSD. In these systems, there were no changes in column operating pressures to achieve heat integration. For THF/water, heat integration reduces energy consumption but significantly increases the reboiler heat duty of the HPC. This increases the exergy inflow into the HPC, consequently increasing the exergy destruction in the HPC, while the separation work, $w_{sep,}$ reduces the exergy loss increases. The heat integration system uses less energy, and this energy is of lower quality to achieve the separation. It is a similar case for the acetone/chloroform system. However, for this system, the global thermodynamic efficiency values are lower because the top streams are the product streams and leave the system at comparably lower temperatures, consequently lower exergy. Also, the small shift in azeotropic composition with changing pressure, as well as the close-boiling nature of the two components, point to the significant separation difficulty of the acetone/chloroform mixture by PSD.

The poor performance of the heat-integrated scheme can be explained further. Heat transfer is more evenly distributed when heat integration is not present. Non-heat-integrated structures consume more energy while also supplying more energy to other processes, and these supplied energies are of greater quality when they exit the system. A further surprising finding in pressure-swing configurations is the higher amount of transiting exergy. This is a result of the integration circuit between the top product of one column and the reboiler of the other column, which is also destroyed partially and recirculated to the former. With the use of such an exergy flux, heat from the top stream of one column may be recovered, and the quantity of the utility steam needed to reboil the bottoms of the other column is decreased. Consequently, the low-pressure column in DHIPSD designs has substantially higher rational efficiency.

A better comparison can be carried out from the lean manufacturing perspective. In this view, all cooling temperatures are T_0 and there is no further integration possibility. The condenser duty is rejected to the ambient atmosphere ($T_c = T_0$). A uniform cooling water supply is used. There is a uniform temperature for the cooling water. This way of operation is realistic for medium standalone plants which may not be integrated with other plants or processes. Repeating the calculation for the systems with a uniform cooling water temperature of 30 °C gives the results shown in Table 8. The table does not include the analysis for the extractive distillation of acetone/chloroform since its heat integration was not beneficial.

Table 8. Thermodynamic efficiency values for the standalone systems.

System	ED Mix 1	DFHIED Mix 1	PSD Mix 1	DFHIPSD Mix 1	PSD Mix 2	DFHIPSD Mix 2
Total exergy destruction (kW)	398.3	290.9	538.5	378.7	5828.4	3935.6
Exergy efficiency (%)	8.7	11.3	17.8	18.9	9.5	10.8

In all the cases, the direct fully heat-integrated schemes have the highest efficiency. This is because, in standalone mode, where there is just the distillation system with no possibility for heat cascade with other processes, heat integration uses less enthalpy, thus saving exergy. The separation efficiency dramatically reduces when the condenser duty is “wasted”. A larger total exergy loss indicates that the separation process is more irreversible and hence less efficient. In using the uniform temperature of utilities, Haragovics and Mizsey [24] found that exergy analysis loses its relevance. This is due to the disappearance of temperature disparities. Since the source of the utilized heat is identical across all scenarios, the variance in exergy loss only results from variations in the amount of the utilized heat. In other words, the exergy balance is reduced to an enthalpy balance in this situation.

From the standpoint of both energy and exergy evaluation, the total reboiler duty is the most significant aspect influencing the requirement of energy, net exergy loss, and thermodynamic efficiency. It can be pointed out that utilizing heat integration within the same process may not always be beneficial, since implementing such integration could involve adjustments that decrease the overall thermodynamic efficiency. Further utilization of the exergy from the cold utility and product streams has the potential to reduce exergy losses in distillation processes, thereby increasing overall thermodynamic efficiency.

5. Conclusions

In this study, the comparison of distillation alternatives for separating equimolar azeotropic binary mixtures of THF/water and acetone/chloroform has been carried out based on the concept of thermodynamic efficiency. This has been accomplished using an exergy assessment that takes into account the global exergy efficiency and exergy destruction rate for each option. This technique allows the determination of the rates and efficiencies of local and global irreversibility, resulting in the following conclusions and insights:

- Except for the extractive distillation of the maximum-boiling acetone/chloroform, full heat integration in both extractive and pressure-swing distillation designs can result in energy savings across all studied systems.
- Surprisingly, heat integration may negatively impact the exergy performance of pressure-swing distillation alternatives while enhancing the exergy performance of extractive distillation systems. These results suggest that the specific form of heat integration employed in this study is economically advantageous for certain mixtures but may not be universally applicable to any arbitrary azeotropic mixture.
- Conducting a comprehensive analysis at the system level is crucial to determining the optimal configuration that maximizes the overall process efficiency. This is a critical step towards making informed decisions in process engineering, as it underscores the nature of distillation separations and the significance of considering both energy and exergy aspects.

These results may be extended for other azeotropes sharing comparable vapor–liquid equilibrium characteristics. By providing an understanding of the effects of heat integration on various distillation configurations, this knowledge enables the selection of the most favorable option for a given mixture, ultimately contributing to more sustainable and efficient industrial processes.

Furthermore, it is crucial to recognize that for a more comprehensive thermodynamic assessment of the systems studied, the analysis should also be expanded to the assessment of dynamic behaviors. This would allow for the detection of transient exergy losses and also facilitate a more comprehensive evaluation of how to improve the design configurations with respect to common operational disturbances.

Supplementary Materials: The following supporting information can be downloaded at: https://www.mdpi.com/article/10.3390/pr12010014/s1, Table S1: Binary interaction parameters for THF/water/DMSO system; Table S2: Binary interaction parameters for acetone/chloroform/DMSO system.

Author Contributions: Conceptualization, P.M. and J.W.M.; methodology, P.M. and J.W.M.; software, J.W.M.; writing—original draft preparation, J.W.M. and G.W.M.; writing—review and editing, P.M., P.S.V. and A.S.; supervision, P.M. and A.S.; project administration, P.M. and P.S.V. Funding acquisition, P.M. and P.S.V. All authors have read and agreed to the published version of the manuscript.

Funding: This research was funded by the Tempus Public Foundation through the Stipendium Hungaricum program, the Hungarian Scientific Research Funds OTKA 128543, and the LIFE19 CCA/HU/001320–LIFE-CLIMCOOP project supported by the EU LIFE program. The EU Sustainable Process Integration Laboratory–SPIL project, funded as project No. CZ.02.1.01/0.0/0.0/15

003/0000456, by Czech Republic Operational Programme Research and Development, Education is also gratefully acknowledged.

Data Availability Statement: The data that support the findings of this study are available from the corresponding authors upon reasonable request.

Conflicts of Interest: The authors declare no conflicts of interest.

Nomenclature

B	Bottom product
D	Distillate product
DHI	Direct heat integrated
EC	Extractive column
ED	Extractive distillation
Ex	Exergy flow [kw]
H	Enthalpy
HPC	High-pressure column
LPC	Low-pressure column
Mix 1	Tetrahydrofuran/water
Mix 2	Acetone/chloroform
m	Mass flow [kg/h]
n	Mole flow [kmol/h]
PSD	Pressure-swing distillation
Q	Heat flow [kw]
QC	Condenser duty [kw]
QR	Reboiler duty [kw]
RR	Molar reflux ratio
S	Entropy
SRC	Solvent recovery column
TC	Cold utility temperature [K]
To, Po	Ambient temperature [K] and pressure [bar]
TR	Hot utility temperature [K]
Wnet	Network consumption of the utility system [kw]
Symbol	
Greek letter	
Δ	Difference
η	Thermodynamic efficiency [%]

References

1. Engelien, H.K.; Larsson, T.; Skogestad, S. Implementation of Optimal Operation for Heat Integrated Distillation Columns. *Chem. Eng. Res. Des.* **2003**, *81*, 277–281. [CrossRef]
2. Yan, J.; Liu, J.; Ren, J.; Wu, Y.; Li, X.; Sun, T.; Sun, L. Design and Multi-Objective Optimization of Hybrid Reactive-Extractive Distillation Process for Separating Wastewater Containing Benzene and Isopropanol. *Sep. Purif. Technol.* **2022**, *290*, 120915. [CrossRef]
3. Yang, A.; Su, Y.; Sun, S.; Shen, W.; Bai, M.; Ren, J. Towards Sustainable Separation of the Ternary Azeotropic Mixture Based on the Intensified Reactive-Extractive Distillation Configurations and Multi-Objective Particle Swarm Optimization. *J. Clean. Prod.* **2022**, *332*, 130116. [CrossRef]
4. You, X.; Rodriguez-Donis, I.; Gerbaud, V. Reducing Process Cost and CO_2 Emissions for Extractive Distillation by Double-Effect Heat Integration and Mechanical Heat Pump. *Appl. Energy* **2016**, *166*, 128–140. [CrossRef]
5. Mtogo, J.W.; Toth, A.J.; Fozer, D.; Mizsey, P.; Szanyi, A. Effects of Energy Intensification of Pressure-Swing Distillation on Energy Consumption and Controllability. *ACS omega* **2022**, *8*, 726–736. [CrossRef] [PubMed]
6. Aurangzeb, M.; Jana, A.K. Pressure-Swing Dividing Wall Column with Multiple Binary Azeotropes: Improving Energy Efficiency and Cost Savings through Vapor Recompression. *Ind. Eng. Chem. Res.* **2018**, *57*, 4019–4032. [CrossRef]
7. Li, X.; Geng, X.; Cui, P.; Yang, J.; Zhu, Z.; Wang, Y.; Xu, D. Thermodynamic Efficiency Enhancement of Pressure-Swing Distillation Process via Heat Integration and Heat Pump Technology. *Appl. Therm. Eng.* **2019**, *154*, 519–529. [CrossRef]
8. Chen, Y.; Liu, C.; Geng, Z. Design and Control of Fully Heat-Integrated Pressure Swing Distillation with a Side Withdrawal for Separating the Methanol/Methyl Acetate/Acetaldehyde Ternary Mixture. *Chem. Eng. Process. Process Intensif.* **2018**, *123*, 233–248. [CrossRef]

9. Li, Y.; Sun, T.; Ye, Q.; Li, J.; Xu, Y.; Jian, X. Application of an Energy-Efficient Process with Reactive Coupling Pressure-Swing Distillation for Recycling Organic Materials from Wastewater. *Ind. Eng. Chem. Res.* **2021**, *60*, 10338–10353. [CrossRef]
10. Linnhoff, B.; Flower, J.R. Synthesis of Heat Exchanger Networks: II. Evolutionary Generation of Networks with Various Criteria of Optimality. *AIChE J.* **1978**, *24*, 642–654. [CrossRef]
11. Chen, Y.; Eslick, J.; Grossmann, I.; Miller, D. Simultaneous Optimization and Heat Integration Based on Rigorous Process Simulations. In *Computer Aided Chemical Engineering*; Eden, M.R., Siirola, J.D., Towler, G.P.B.T.-C.A.C.E., Eds.; Elsevier: Amsterdam, The Netherlands, 2014; Volume 34, pp. 477–482. [CrossRef]
12. Yin, M.; Hua, C.; Lu, P.; Zhang, H.; Bai, F. Design and Control of Pressure-Swing Heat Integration Distillation for the Trichlorosilane Purification Process. *ACS Omega* **2022**, *7*, 9254–9266. [CrossRef] [PubMed]
13. Zhai, J.; Chen, X.; Sun, X.; Xie, H. Economically and Thermodynamically Efficient Pressure-Swing Distillation with Heat Integration and Heat Pump Techniques. *Appl. Therm. Eng.* **2023**, *218*, 119389. [CrossRef]
14. Duan, C.; Li, C. Energy-Saving Improvement of Heat Integration for Separating Dilute Azeotropic Components in Extractive Distillation. *Energy* **2023**, *263*, 125821. [CrossRef]
15. Li, X.; Ye, Q.; Li, J.; Liu, Y.; Yan, L.; Jian, X.; Zhang, J. Investigation on Energy-Efficient Heterogeneous Pressure-Swing Azeotropic Distillation for Recovery of Cyclohexane and Tert-Butanol from Industrial Effluent. *Sep. Purif. Technol.* **2023**, *306*, 122705. [CrossRef]
16. Mtogo, J.W.; Toth, A.J.; Szanyi, A.; Mizsey, P. Comparison of Controllability Features of Extractive and Pressure Swing Distillations on the Example of Tetrahydrofuran Dewatering. *ACS Omega* **2021**, *6*, 35355–35362. [CrossRef] [PubMed]
17. Zhang, Y.R.; Wu, T.W.; Chien, I.L. Energy-Efficient Heterogeneous Azeotropic Distillation Coupling with Pressure Swing Distillation for the Separation of IPA/DIPE/Water Mixture. *J. Taiwan Inst. Chem. Eng.* **2022**, *130*, 103843. [CrossRef]
18. Zhang, F.; Sun, D.; Li, Y.; Shan, B.; Ma, Y.; Wang, Y.; Li, X.; Zhu, Z. Heat Integration and Dynamic Control for Separating the Ternary Azeotrope of Butanone/Isopropanol/n-Heptane via Pressure-Swing Distillation. *Chem. Eng. Process. Intensif.* **2022**, *170*, 108657. [CrossRef]
19. Ozturk, M. Energy and Exergy Analysis of a Combined Ground Source Heat Pump System. *Appl. Therm. Eng.* **2014**, *73*, 362–370. [CrossRef]
20. Arslanoglu, N. Development of Empirical Models for Estimation Diffuse Solar Radiation Exergy in Turkey. *Int. J. Exergy* **2022**, *37*, 24–39. [CrossRef]
21. Zemp, R.J.; De Fana, S.H.B.; Oliveira Maia, M.D.L. Driving Force Distribution and Exergy Loss in the Thermodynamic Analysis of Distillation Columns. *Comput. Chem. Eng.* **1997**, *21* (Suppl. S1), S523–S528. [CrossRef]
22. Sauar, E.; Siragusa, G.; Andresen, B. Equal Thermodynamic Distance and Equipartition of Forces Principles Applied to Binary Distillation. *J. Phys. Chem. A* **2001**, *105*, 2312–2320. [CrossRef]
23. Ashrafizadeh, S.A.; Amidpour, M.; Abolmashadi, M. Exergy Analysis of Distillation Column Using Concept of Driving Forces. *J. Chem. Eng. Japan* **2013**, *46*, 434–443. [CrossRef]
24. Haragovics, M.; Mizsey, P. A Novel Application of Exergy Analysis: Lean Manufacturing Tool to Improve Energy Efficiency and Flexibility of Hydrocarbon Processing. *Energy* **2014**, *77*, 382–390. [CrossRef]
25. Demirel, Y. Thermodynamic Analysis of Separation Systems. *Sep. Sci. Technol.* **2004**, *39*, 3897–3942. [CrossRef]
26. Yuan, B.; Yang, Z.; Yang, A.; Tao, J.; Ren, J.; Wei, S.; Shen, W. Target Localization Optimization of a Superstructure Triple-Column Extractive Distillation with Four-Parallel Evaporator Organic Rankine Cycles System Based on Advanced Exergy Analysis. *Sep. Purif. Technol.* **2021**, *272*, 118894. [CrossRef]
27. Javed, A.; Hassan, A.; Babar, M.; Azhar, U.; Riaz, A.; Mujahid, R.; Ahmad, T.; Mubashir, M.; Lim, H.R.; Show, P.L.; et al. A Comparison of the Exergy Efficiencies of Various Heat-Integrated Distillation Columns. *Energies* **2022**, *15*, 6498. [CrossRef]
28. Guerrero-Martin, C.A.; Fernández-Ramírez, J.S.; Arturo-Calvache, J.E.; Milquez-Sanabria, H.A.; da Silva Fernandes, F.A.; Costa Gomes, V.J.; e Silva, W.; Dutra Valente Duarte, E.; Guerrero-Martin, L.E.; Lucas, E.F. Exergy Load Distribution Analysis Applied to the Dehydration of Ethanol by Extractive Distillation. *Energies* **2023**, *16*, 3502. [CrossRef]
29. Zhao, J.; Zhang, Y.; Qi, H.; Li, X.; Zhu, Z.; Wang, Y.; Cui, P.; Gao, J. Process Design and Intensification for the Clean Separation of Ternary Multi-Azeotropes System via Special Distillation Coupled with Reaction. *J. Clean. Prod.* **2021**, *328*, 129520. [CrossRef]
30. Mangili, P.V.; Maia, M.P. Comparison of the Exergetic Performance and CO2 Emissions of Tetrahydrofuran-Water Separation Processes. *Chem. Eng. Process. Intensif.* **2020**, *147*, 107748. [CrossRef]
31. Ghuge, P.D.; Mali, N.A.; Joshi, S.S. Comparative Analysis of Extractive and Pressure Swing Distillation for Separation of THF-Water Separation. *Comput. Chem. Eng.* **2017**, *103*, 188–200. [CrossRef]
32. Xu, Q.; Wang, Z.; Dai, Y.; Zhao, Q.; Li, Y.; Cui, P.; Zhu, Z.; Wang, Y.; Gao, J.; Ma, Y. Economy, Exergy, Energy Consumption and Environmental Human Toxicity Potential Assessment of Vacuum Extractive Distillation Coupled Pervaporation Process for Separating Acetone/Isopropanol/Water Multi-Azeotropes System. *Sep. Purif. Technol.* **2022**, *300*, 121834. [CrossRef]
33. Tang, W.T.; Ward, J.D. Energy and Exergy Analysis of a Stacked Complex Sequence and Alternatives for Ternary Distillation. *Sep. Purif. Technol.* **2023**, *304*, 122384. [CrossRef]
34. Araújo, A.B.; Brito, R.P.; Vasconcelos, L.S. Exergetic Analysis of Distillation Processes—A Case Study. *Energy* **2007**, *32*, 1185–1193. [CrossRef]
35. Le Goff, P.; Cachot, T.; Rivero, R. Exergy Analysis of Distillation Processes. *Chem. Eng. Technol.* **1996**, *19*, 478–485. [CrossRef]

36. Yan, C.; Lv, L.; Wei, S.; Eslamimanesh, A.; Shen, W. Application of Retrofitted Design and Optimization Framework Based on the Exergy Analysis to a Crude Oil Distillation Plant. *Appl. Therm. Eng.* **2019**, *154*, 637–649. [CrossRef]
37. Rivero, R.; Anaya, A. Exergy Analysis of Industrial Processes: Energy-Economy-Ecology. *Lat. Am. Appl. Res.* **1997**, *27*, 191–205.
38. Ognisty, T.P. Analyze Distillation Columns with Thermodynamics. *Chem. Eng. Prog.* **1995**, *91*, 40–46.
39. Schuldt, K.; Brinkmann, T.; Georgopanos, P. Zero-Discharge Process for Recycling of Tetrahydrofuran–Water Mixtures. *Processes* **2021**, *9*, 729. [CrossRef]
40. Luyben, W.L. Comparison of Flowsheets for THF/Water Separation Using Pressure-Swing Distillation. *Comput. Chem. Eng.* **2018**, *115*, 407–411. [CrossRef]
41. Zhang, Z.; Huang, D.; Lv, M.; Jia, P.; Sun, D.; Li, W. Entrainer Selection for Separating Tetrahydrofuran/Water Azeotropic Mixture by Extractive Distillation. *Sep. Purif. Technol.* **2014**, *122*, 73–77. [CrossRef]
42. Gu, J.; You, X.; Tao, C.; Li, J.; Shen, W.; Li, J. Improved Design and Optimization for Separating Tetrahydrofuran–Water Azeotrope through Extractive Distillation with and without Heat Integration by Varying Pressure. *Chem. Eng. Res. Des.* **2018**, *133*, 303–313. [CrossRef]
43. Hostrup, M.; Harper, P.M.; Gani, R. Design of Environmentally Benign Processes: Integration of Solvent Design and Separation Process Synthesis. *Comput. Chem. Eng.* **1999**, *23*, 1395–1414. [CrossRef]
44. Luyben, W.L. Comparison of Extractive Distillation and Pressure-Swing Distillation for Acetone/Chloroform Separation. *Comput. Chem. Eng.* **2013**, *50*, 1–7. [CrossRef]
45. Wang, Y.-H.; Chien, I.-L. Unique Design Considerations for Maximum-Boiling Azeotropic Systems via Extractive Distillation: Acetone/Chloroform Separation. *Ind. Eng. Chem. Res.* **2018**, *57*, 12884–12894. [CrossRef]
46. Yang, D.; Zhang, Q.; Zhang, Q.; Cui, C. Dynamics and Control of Electrified Pressure-Swing Distillation for Separating a Maximum-Boiling Azeotrope Featuring Small Pressure-Induced Shift. *Sep. Purif. Technol.* **2023**, *312*, 123360. [CrossRef]
47. Cao, Y.; Hu, J.; Jia, H.; Bu, G.; Zhu, Z.; Wang, Y. Comparison of Pressure-Swing Distillation and Extractive Distillation with Varied-Diameter Column in Economics and Dynamic Control. *J. Process Control* **2017**, *49*, 9–25. [CrossRef]
48. Kotas, T.J. *The Exergy Method of Thermal Plant Analysis*; Paragon Publishing: Trowbridge, UK, 2012.
49. Hinderink, A.P.; Kerkhof, F.P.J.M.; Lie, A.B.K.; De Swaan Arons, J.; Van Der Kooi, H.J. Exergy Analysis with a Flowsheeting Simulator—I. Theory; Calculating Exergies of Material Streams. *Chem. Eng. Sci.* **1996**, *51*, 4693–4700. [CrossRef]